Photochemical & Photobiological Sciences

PAPER

Cite this: *Photochem. Photobiol. Sci.*, 2014, **13**, 1469

Co-assembly and luminescence tuning of hybrids with task-specified ionic liquid encapsulating and linking lanthanide-polyoxometalates and complexes†

Bing Yan* and Jing Cuan

Received 8th April 2014,
Accepted 20th July 2014

DOI: 10.1039/c4pp00125g

www.rsc.org/pps

A class of novel multifunctional hybrids assembled by lanthanide polyoxometalates, ionic liquid and lanthanide complexes were prepared through the reactions of ion exchange and coordination in mild conditions. These hybrids possess two luminescence centers, one is lanthanide polyoxometalates ($[EuW_{10}O_{36}]^{9-}$ or $[TbW_{10}O_{36}]^{9-}$), the other is lanthanide complexes of 1,10-phenanthroline (phen) (or 2,2′-bipyridine (bpy)) and ionic liquid (1-methyl-3-propionic imidazole unit). Fourier transform infrared (FTIR) spectra, X-ray diffraction (XRD) analysis, thermo-gravimetric analysis (TGA), UV/vis diffuse reflectance spectra and photoluminescent properties are utilized to characterize these hybrid materials. The results reveal that all hybrids possess amorphous microstructures and are composed of inorganic polyoxometalates and lanthanide nitrate through chemical bonds. Most hybrids exhibit outstanding luminescent properties such as high quantum efficiency and long lifetimes. Moreover, the luminescent color of them can be tuned and even the white luminescence can be integrated.

Introduction

Lanthanide complexes are outstanding and important in the fields of luminescent materials. In recent years, they have aroused continuous attention in design of tunable solid-state lasers,[1] optical amplification,[2] optical sensors,[3] light-conversion molecular devices,[4] analytical and structural probes in material science.[1a,5] As is well known, the molar absorption coefficients of trivalent lanthanide ions are very little and most of them suffer from weak absorption.[6] However, the study of lanthanide complex made up for this as the result of intense absorption of some organic ligands typically in the ultraviolet or visible spectral region[7] and the effective intramolecular energy transfer process (so-called antenna effect). Certain organic ligands like β-diketone derivatives,[3,8] aromatic carboxylic acids,[9] heterocyclic ligands[8c,10] and macrocyclic ligands possess coordination sites[11] (oxygen or nitrogen atoms) and conjugated structures, which are often useful units to build lanthanide complexes. Polyoxometalates are clusters constructed by some transition metals in their highest valency and oxygen atoms. Their elegant and certain molecular structures, diverse intra-electron configuration, nanoscale sizes are valuable properties.[11] They are chosen as useful inorganic building blocks for functionalized hybrids for their advantages: Firstly, different polyoxometalates anions have their own characteristics in charge, molecular shapes, sizes and it is possible to design a variety of compounds in different spatial forms by the interaction between polyoxometalates and organic components. Secondly, polyoxometalates possess the structure of high symmetry, which can dissolve in water and other polar organic solvent without changing its structures. Thus, we can obtain the target products by different ways. Thirdly, the polyoxometalates can be used as electron acceptor, which is able to combine with organic donors containing N, S, and O atoms. This will be reduced to mixed valence anion, thus forming the charge transfer complexes. Among the well-known lanthanide-containing polyoxometalates, the europium decatungstate or decatungstoeuropate (9–) anion $[EuW_{10}O_{36}]^{9-}$ exhibits the best luminescence performance, whose quantum efficiency can reach above 50%. Decatungstoeuropate anion is one of the Lindquist-type polyoxometalates, consisting two $[W_5O_{18}]^{6-}$ fragments that coordinate to central europium ions with oxygen atoms. Many studies[12] have reported the assembly of $Na_9EuW_{10}O_{36}{\cdot}32H_2O$ into organic–inorganic hybrids through the electrostatic force between $[EuW_{10}O_{36}]^{9-}$ anion and cationic surfactants like dimethyldioctadecylammonium, dodecyltrimethylammonium and hexadecyltrimethylammonium. In our work, we select task-specified ionic liquid to encapsulate decatungstoeuropate (9–) anion by the same principle. Task-specified

Department of Chemistry, Tongji University, Shanghai, 200092, China. E-mail: byan@tongji.edu.cn; Tel: +86-21-65984663

†Electronic supplementary information (ESI) available. See DOI: 10.1039/c4pp00125g

ionic liquid refers to certain ionic liquid that contains the active functional groups, such as amino,[13] thiol,[14] terpyridyl,[15] carboxyl,[16] and alkoxy.[17] This kind of ionic liquid possesses two characteristics. On the one hand, the end with positive charges can adsorb polyoxometalates anion and on the other hand, the active groups can be used for series of functionalization reactions.

In this work, the task-specified ionic liquid, 1-methyl-3-propionic imidazole bromide is utilized to assemble luminescent hybrids. The imidazole cation is used to encapsulate europium polyoxometalates, while the propionic group coordinates to trivalent lanthanide ions (Eu^{3+}, Tb^{3+}) and 1,10-phenanthroline (phen)/2,2′-bipyridine (bpy) behaves as a second ligand. The physical characterization and especially photoluminescent properties of these hybrids are discussed in detail.

Experimental section

Materials

Europium and terbium nitrate were obtained by dissolving their metal oxides in concentrated nitric acid. Heating was stopped when the solution became viscous and stirring was continued till the solution became dry. $Na_2WO_4{\cdot}2H_2O$, 3-bromopropionic acid, 1-methyl-imidazole, 1,10-phenanthroline (phen), 2,2′-bipyridine (bpy) were from Aldrich. All reagents were used as obtained without further purification.

Synthetic procedures

The preparations of europium polyoxometalates and terbium polyoxometalates. $Na_9LnW_{10}O_{36}{\cdot}32H_2O$ was abbreviated as LnW10, in which Ln = Eu, Tb, and its classical synthesis method follows that of Peacock and Weakley.[18] Firstly, 10 mmol $Na_2WO_4{\cdot}2H_2O$ (3.3 g) was dissolved in 8 mL deionized water, and then the solution was heated to 85 °C. Glacial acetic acid was used to adjust the pH to about 7. After that, 0.8 mL europium nitrate solution containing 1 mmol europium nitrate was added slowly into the above solution. We could observe lots of white precipitates appeared at once, and stop heating after adding europium nitrate solution. The whole solution was cooled down in an ice water bath. The europium polyoxometalates (denoted as EuW10) were obtained after filtration and washed with ethanol two times, and then dried in air. The synthesis of terbium polyoxometalates (TbW10) was following similar way by replacing europium nitrate with terbium nitrate, and the molar amount was not changed.

Synthesis of task-specified ionic liquid (denoted as IM^+Br^-). The task-specified ionic liquid was synthesized using the reported method of Li.[19] Firstly, 100 mmol 3-bromopropionic acid was dissolved in ethanol (10 mL) and equimolar amount of 1-methyl-imidazole was added dropwise to the solution. The mixture was stirred under refluxing at 75 °C for 8 hours and pale-yellowish viscous ionic liquid was acquired. The original crude ionic liquid was washed with Et_2O for several times, and the solvent was evaporated by the rotary vacuum evaporator. The purified ionic liquid was obtained and denoted as IM^+Br^-. 1H NMR (400 MHz, DMSO-d^6): δ(9.17, s, 1H), δ(7.79, s, 1H), δ(7.66, s, 1H), δ(4.36, t, 2H), δ(2.91, t, 2H), δ(3.87, s, 3H).

The synthesis of luminescent hybrids EuW10-IL-Eu-phen. Firstly, 0.9 mmol IM^+Br^- was dispersed in 20 mL absolute ethanol, and then 0.3 mmol phen and 0.3 mmol europium nitrate was added into the above solution. Then, the mixed solution was stirred and heated at 40 °C for 12 hours to perform the coordinating reaction. After this reaction, several drops of triethylamine were used to adjust the pH to 7–8, then 0.1 mmol europium polyoxometalates (EuW10) was added into the mixed solution, and the whole solution was heated to 70 °C to react for 24 hours. The hybrids were purified by centrifugation and washed with cyclohexane for several times. The final product was dried and denoted as EuW10-IL-Eu-phen. Its predicted structure is shown in Fig. 1. By the similar methods, replacing EuW10 with TbW10, TbW10-IL-Eu-phen hybrids can be obtained. By the same principle, we can prepare EuW10-IL-Tb-phen by changing europium nitrate with terbium nitrate. Note that TbW10-IL-Tb-phen was prepared by replacing both EuW10 and europium nitrate with TbW10 and terbium nitrate by following the above procedure.

The synthesis of luminescent hybrids EuW10-IL-Eu-bpy. Firstly, 0.9 mmol IM^+Br^- was dispersed in 20 mL absolute ethanol, and then 0.3 mmol bpy and 0.3 mmol europium nitrate was added into the above solution. Then, the mixed solution was stirred and heated at 40 °C for 12 hours to perform the coordinating reaction. After this reaction, several drops of triethylamine were used to adjust the pH to 7–8. Then, 0.1 mmol europium polyoxometalates (EuW10) was added into the mixed solution, and the whole solution was heated to 70 °C to react for 24 hours. The hybrids were purified by centrifugation and washed with cyclohexane for several times. The final product was dried and denoted as EuW10-IL-Eu-phen. By using a similar method, we obtained TbW10-IL-Eu-phen. Moreover, by the same principle, we can prepare EuW10-IL-Tb-phen by changing europium nitrate with terbium nitrate. TbW10-IL-Tb-phen was prepared by replacing both EuW10 and europium nitrate with TbW10 and terbium nitrate following the above procedure.

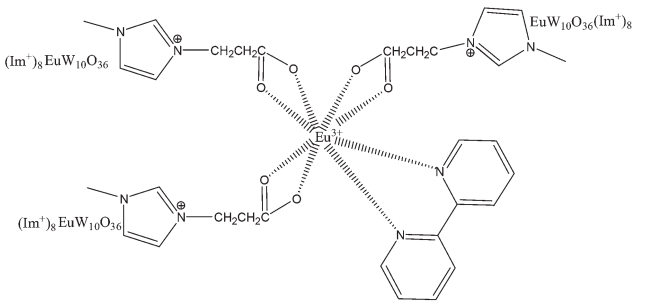

Fig. 1 The selected predicted structure of EuW10-IL-Eu-phen, other hybrids show similar composition except for different lanthanide ions or bpy ligand.

Physical characterization

Fourier transform infrared (FTIR) spectra were measured on a Nexus 912 AO446 spectrophotometer within the 4000–400 cm^{-1} region through the KBr pellet technique. X-ray diffraction analysis was recorded in a 2θ range from 0.6°–6° on a Rigaku D/max-rB diffractometer equipped with a Cu anode. Thermo-gravimetric analysis (TGA) was performed under nitrogen atmosphere using Netzsch STA 409 by placing samples in Al_2O_3 crucibles at the heating rate of 15 °C min^{-1} from 30 to 1000 °C. The UV/vis diffuse reflectance spectra were obtained with the BWS003 spectrophotometer. Both excitation/emission spectra and luminescence lifetime measurements were obtained on the Edinburgh FLS920 phosphorimeter using a 450 W xenon lamp as the excitation source at room temperature. The luminescent quantum efficiency was acquired using an integrating sphere (150 mm diameter, $BaSO_4$ coating) with the Edinburgh FLS920 phosphorimeter. The luminescence spectra were corrected for variations in the output of the excitation source and for variations in the detector response.

Results and discussion

The whole hybrid system is composed by two kinds of luminescent lanthanide units through IM^+Br^- as double functional linker: one is lanthanide polyoxometalate and the other is lanthanide complexes. Here, IM^+Br^- interacts with lanthanide polyoxometalate unit through ionic exchange between IM^+ and LnW_{10}^{9-} and link lanthanide complexes of phen or bpy through the coordination reaction between the carboxylate group of IM^+ and lanthanide ion for the high coordination number of Ln^{3+}. Subsequently, the two kinds of luminescent lanthanide species can be assembled into one hybrid system, whose typical scheme is shown in Fig. 1.

The FTIR spectra of task-specified ionic liquid IM^+Br^-, four phen hybrids, and four bpy hybrids are shown in Fig. S1(A), (B) and (C),† respectively. In Fig. S1(A),† the absorption peak locating at 3100 cm^{-1} is assigned to the stretching vibration of C–H on the imidazole ring and the aliphatic chain. The ν(C–O, C═O) for COOH of IM^+Br^- is located at 1168 cm^{-1} and 1730 cm^{-1}, respectively.[20] However, these two peaks disappear in Fig. S1(B),† and new peaks centered at 1591, 1570 cm^{-1}, which correspond to the asymmetric stretching vibration of carboxylate coming into being. During this process, the coordination reactions between carboxyl group and lanthanide ions lead to the loss of proton and oxygen atoms linked to lanthanide ions by coordination bond. At the same time, the skeleton stretching vibration peaks of neutral ligand red-shift to higher wavenumber, which suggest that nitrogen atoms also take part in the coordination reaction of lanthanide ions.[21] Fig. S1(C)† shows us the infrared information of bpy hybrids. Moreover, the peaks at 1168 cm^{-1} and 1730 cm^{-1} of carboxyl group disappear and new peaks arise at 1627 and 1578 cm^{-1}, which can be ascribed to the asymmetric stretching vibration of carboxylate. This proves the success of coordination reaction between carboxyl group and lanthanide ions. At the same time, as the result of coordination between nitrogen atoms and lanthanide ions, the skeleton peaks of bpy red shift.[22]

To study the thermal stability of obtained materials, we take the test of thermal gravimetric analysis and differential of thermal gravimetric analysis for EuW10-IL-Eu-bpy/EuW10-IL-Eu-phen hybrids. Their heat endurance ability can be seen in the curves of Fig. S2(a) and (b).† In Fig. S2(a),† we can observe three weight loss processes. The first weight loss is of 2.0% in the range of 30–111 °C, which is caused by the evaporation of physical absorbed water and the remaining solvent ethanol.[23] The second weight loss of about 6.8% begins at 111 °C and lasts to 210 °C, and it is mainly caused by the loss of water of crystallization of lanthanide polyoxometalates.[24] The last weight loss is about 13% in the range of 210–516 °C, which is the result of the breakage of Ln–O and Ln–N coordination bonds, the decomposition of ionic liquid, the collapse of organic skeleton in **2**, bpy ligands and the final residues are mainly Eu_2O_3, polyoxometalates. Fig. S2(b)† shows us the heat endurance ability of EuW10-IL-Eu-phen. There are also three weight changing regions. The first weight changing process is below 202 °C (weight loss of 4.3%). Note that the physically absorbed water, remaining solvent, water of crystallization of lanthanide polyoxometalates evaporated, which caused this weight changing process. During the second weight loss in the region of 202–279 °C, most of crystal water in lanthanide polyoxometalates is removed. The last weight loss from 279 to 1000 °C is mainly caused by the rupture of coordination bond, which led to the decomposition of phen, and the final residues are Eu_2O_3, polyoxometalates.

The UV-vis diffuse reflection absorption spectra are measured in powder for all the obtained hybrid materials. Fig. S3(a)† shows the UV-vis diffuse reflection absorption spectra of four bpy hybrid materials. In this spectra, we can observe that there is a broad and strong absorption bond centered at about 300 nm, which is mainly caused by the $\pi \rightarrow \pi^*$ transitions of bpy and the skeleton absorption of polyoxometalates, but the positions of this central broad absorption band red shift. This is because the generation of Ln–N coordination bonds led to the expansion of the conjugate range. Some of the absorption peaks in UV-vis diffuse reflection absorption spectra overlap with that of luminescence excitation spectra below. At the same time, we can also observe some obvious inverse peaks in the absorption spectra. This is the result of sensitization of lanthanide ions. The inverse peaks are mainly caused by the characteristic emission of Eu^{3+} and Tb^{3+} when the hybrid materials are excited by UV light shining and the efficient intramolecular transfer, which is the so-called antenna effect. Through the data of UV-vis diffuse absorption spectra, we can primarily predict these four bpy hybrid materials may possess outstanding luminescent properties. In the UV-vis diffuse absorption spectra of four phen hybrid materials, we can see similar broad absorption bands in the range of 250–400 nm. For these four hybrid materials, an obvious red shift of the absorption bands is observed. This may be due to the generation of Ln–N coordination bonds, leading to the expansion of the conjugate range. In the region

about 400 nm, some weak inverse peaks representing f–f transitions of Eu^{3+} can also be observed. We can conclude that, lanthanide ions in these materials can be effectively sensitized through antenna effect. Their detailed luminescence information will be further discussed later combined with the luminescence excitation and emission spectra of these hybrid materials.

Fig. S4(a) and (b)† show the X-ray diffraction analysis of the 2,2′-bpy hybrid materials and phen hybrid materials from 10°–70° in a 2θ range. The X-ray diffraction analysis curves of these two class hybrid materials are similar in shapes, and a broad weak band centered at 30° is shown, which is characteristic of amorphous structures.[25] No high intensity peaks of crystal materials can be found in the figures; *i.e.*, no free lanthanide polyoxometalates or lanthanide inorganic compounds exist in the whole materials, and the whole materials are in homogenous organic–inorganic systems, which are constructed by strong chemical bonds.

To investigate the luminescent behaviors of these obtained eight organic–inorganic hybrids, we measured both the excitation and emission spectra of them. For the convenience to discuss, we classify for 4 groups according to criteria of both same lanthanide and same bridge lanthanide ions. Firstly, Fig. 2(a) and (b) show us the excitation and emission spectra of EuW10-IL-Eu-phen/EuW10-IL-Eu-bpy respectively. Their excitation spectra are acquired under the excitation of largest emission wavelength 614 nm. The excitation spectra are similar, and there exist the narrow characteristic peaks of Eu^{3+} and a broad band ranging from about 250 to 350 nm. The relative intensity of broad band is stronger than that of Eu^{3+} characteristic peaks. The broad band is mainly caused by the ligands–metal charge transfer (LMCT) of O→W/O→Eu and π→π* transitions of organic ligands.[7] In EuW10-IL-Eu-phen hybrids, the excitation center of broad band is at 350 nm, while for EuW10-IL-Eu-bpy hybrids, the excitation center of broad band is at 315 nm. This difference is mainly caused by different excitation of organic ligand. Among all Eu narrow characteristic transitions, peaks centered at 395 nm of the $^7F_0 \rightarrow {}^5L_6$ transition are more obvious. Their emission spectra provide us more detailed information about the process of inner energy transfer between different building units inside the molecules. In Fig. 2(b), five primary peaks, located at 581, 592, 614, 649 and 702 nm, can be seen, and these peaks are ascribed to $^5D_0 \rightarrow {}^7F_J$ (J = 0, 1, 2, 3, 4) transitions, respectively. The strongest peak is $^5D_0 \rightarrow {}^7F_2$ transitions. As is well known, $^5D_0 \rightarrow {}^7F_1$ transition belongs to the magnetic dipole transition, which is free from the changing environment of central Eu^{3+}, and it is often used as a criterion in the emission spectra. $^5D_0 \rightarrow {}^7F_2$ transition is ascribed to the electric dipole transition, which is sensitive to changing environment of central Eu^{3+}. The relative intensity ratio (I) ($^5D_0 \rightarrow {}^7F_2$ transition/$^5D_0 \rightarrow {}^7F_1$ transition) is defined as a measurement to evaluate the symmetry of chemical environment around europium. The big values of I suggests that the central europium ion locates the low symmetry site. Calculation of the data of I, we can conclude that, in EuW10-IL-Eu-phen/EuW10-IL-Eu-bpy hybrid materials, Eu^{3+} is situated at a low symmetry site. Through comparison of the relative intensity of EuW10-IL-Eu-phen and EuW10-IL-Eu-bpy hybrid materials, the intensity of EuW10-IL-Eu-phen is higher than that of EuW10-IL-Eu-bpy. This suggests phen is more sensitive for the emission of these materials than 2,2′-bpy ligands.

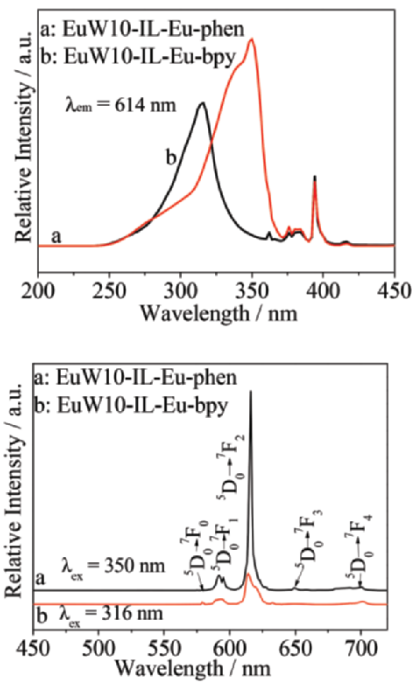

Fig. 2 The excitation and emission spectra of EuW10-IL-Eu-phen/EuW10-IL-Eu-bpy.

Fig. 3(a) and (b) show the excitation and emission spectra of EuW10-IL-Tb-phen and EuW10-IL-Tb-bpy, respectively. In their excitation spectra, we can observe a broad band around 20–350 nm and series of characteristic lanthanide peaks. The intensity of broad band excitation peaks is stronger than that of lanthanide ion's characteristic peaks. Moreover, the center of broad band is located at a farther wavelength in EuW10-IL-Tb-phen than in EuW10-IL-Tb-bpy hybrid materials, similar to that in Fig. 2(a). In their emission spectra, we can observe seven peaks, which are located at 489, 544, 579, 593, 614(619), 649 and 700 nm, respectively and they are the result of overlap of $^5D_4 \rightarrow {}^7F_J$ (J = 6, 5, 4, 3) transitions and $^5D_0 \rightarrow {}^7F_J$ (J = 0, 1, 2, 3, 4) transitions. The relative intensity of $^5D_0 \rightarrow {}^7F_2$ transition is stronger than $^5D_0 \rightarrow {}^7F_1$ transition in EuW10-IL-Tb-phen hybrids, and the ratio is opposite in EuW10-IL-Tb-bpy hybrids; *i.e.*, Eu^{3+} is located at a low symmetry site in EuW10-IL-Tb-phen, while in EuW10-IL-Tb-bpy it is located at a high symmetry site.

Fig. 4(a) and (b) show the excitation and emission spectra of TbW10-IL-Eu-phen and TbW10-IL-Eu-bpy, respectively. In their excitation spectra, we can see a broad band and series of lanthanide characteristic peaks. In TbW10-IL-Eu-bpy, the intensity of Eu^{3+} characteristic peaks is higher than that of the broad band excitation; moreover, in TbW10-IL-Eu-phen, the broad band excitation is stronger than Eu^{3+} characteristic

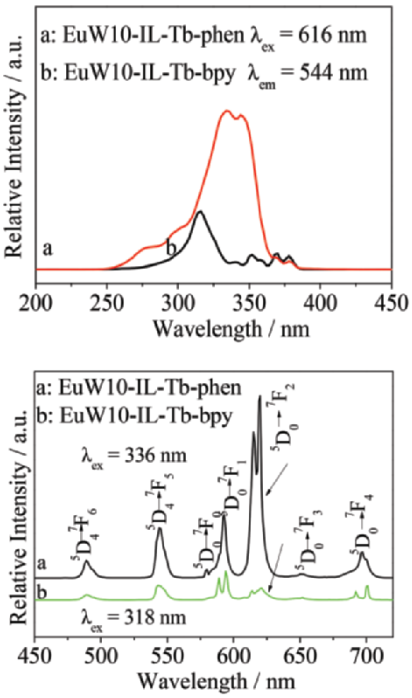

Fig. 3 The excitation and emission spectra of EuW10-IL-Tb-phen/EuW10-IL-Tb-bpy.

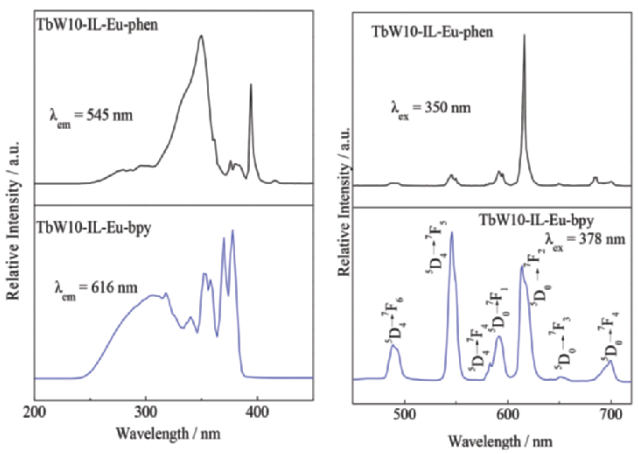

Fig. 4 The excitation and emission spectra of TbW10-IL-Eu-phen/TbW10-IL-Eu-bpy.

peaks. Their emission spectra are same in the positions of emission peaks, but are different in the relative intensities. In TbW10-IL-Eu-phen hybrid materials, $^5D_0 \rightarrow {}^7F_2$ transition of europium ions is the most prominent, while in TbW10-IL-Eu-bpy, the highest peak is the $^5D_4 \rightarrow {}^7F_5$ transition of terbium polyoxometalates; *i.e.*, the introduction of phen can increase the emission ability of europium ions; therefore, the $^5D_0 \rightarrow {}^7F_2$ transition of europium ions is the most prominent. However, bpy is not as effective as phen in sensitizing europium ions emission; thus, in TbW10-IL-Eu-bpy hybrid materials, the relative intensity of europium ions characteristic emission is as low as that of terbium polyoxometalates.

Fig. 5(a) and (b) show us the luminescence information of TbW10-IL-Tb-bpy and TbW10-IL-Tb-bpy hybrid materials, and in the excitation spectra of TbW10-IL-Tb-bpy, we can observe a broad band around 300 nm and strong narrow peaks of lanthanide ions. The relative intensity of lanthanide ions transition in TbW10-IL-Tb-bpy is stronger than in other seven hybrids, and its intensity even exceeds the intensity of matrix and organic ligand transitions. In the excitation spectra of TbW10-IL-Tb-phen, the highest peak is centered at 325 nm, which can be ascribed to the O→W and π→π* transitions of phen, and the former are stronger. The emission spectra of TbW10-IL-Tb-phen and TbW10-IL-Tb-bpy are obtained by exciting at the wavelength of 330 nm and 378 nm, respectively, and we can observe four featured sharp characteristic emission peaks of the $^5D_4 \rightarrow {}^7F_{6,5,4,3}$ transitions, which are located at 490, 545, 587, and 622 nm, respectively. Among these peaks, the $^5D_4 \rightarrow {}^7F_5$ transition is the strongest. These peaks are caused by both terbium polyoxometalates and terbium ions emission. The intensity of emission peaks in TbW10-IL-Tb-bpy hybrids is stronger than that in TbW10-IL-Tb-phen. This may be due to the condition that the triplet-state energies[7,26] of bpy ligand are more suitable than phen ligand for the resonant emitting levels of Tb^{3+}.

The typical decay curves of these eight hybrid materials are tested. They can be described as a single exponential ($\mathrm{Ln}(S(t)/S0) = -k_1 t = -t/\tau$), indicating that all Eu^{3+} and Tb^{3+} ions occupy the same average coordination environment. In hybrids, EuW10-IL-Tb-phen, EuW10-IL-Tb-bpy, TbW10-IL-Eu-phen and TbW10-IL-Eu-bpy, there are two kinds of lanthanide

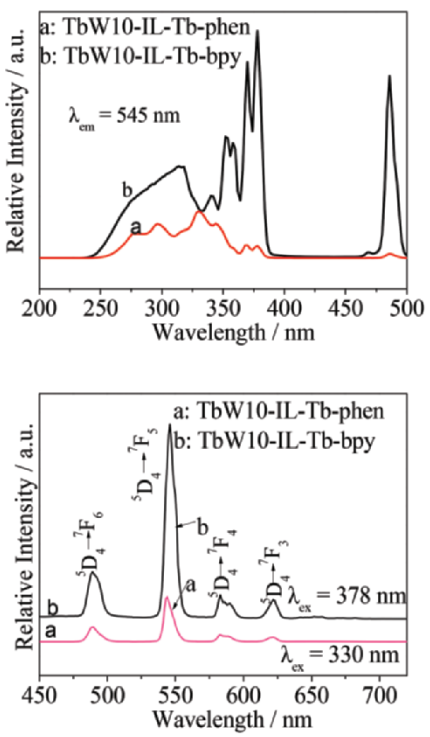

Fig. 5 The excitation and emission spectra of TbW10-IL-Tb-phen/TbW10-IL-Tb-bpy.

ions, containing two decay lifetimes of both $^5D_0$(Eu) and $^5D_4$(Tb) excited states. The resultant $^5D_0$(Eu) excited state decay lifetime of the above four materials are 1084, 1258, 892 and 448 μs, indicating that the $^5D_0$(Eu) excited state decay lifetime of europium polyoxometalates hybrids is longer than that of europium ions hybrids. In these four hybrids, the decay lifetimes of $^5D_4$(Tb) excited state are 169, 1132, 384 and 486 μs, respectively, suggesting that in these Eu/Tb co-fabricated materials, bpy complex hybrids show stronger decay lifetime of $^5D_4$(Tb) excited state. Note that there is only one kind of lanthanide element piece in other four hybrid materials EuW10-IL-Eu-phen, EuW10-IL-Eu-bpy, TbW10-IL-Tb-phen, and TbW10-IL-Tb-bpy, respectively; therefore, they present sole decay lifetimes. The $^5D_0$(Eu) excited state decay lifetimes of EuW10-IL-Eu-phen and EuW10-IL-Eu-bpy are 1095 and 590 μs, respectively. Moreover, the $^5D_4$(Tb) excited state decay lifetimes of TbW10-IL-Tb-phen and TbW10-IL-Tb-bpy are 1064 and 322 μs, respectively. Seeing from above data, we can conclude that for these sole lanthanide piece assembled hybrids, phen hybrids show longer lifetime than bpy hybrids.

The outer luminescent quantum efficiency of these eight luminous hybrids are measured using an integrating sphere (150 mm diameter, $BaSO_4$ coating). The obtained data of luminescent quantum efficiency are listed in Table 1. The parent europium polyoxometalates show better luminescent property (higher quantum efficiency, longer decay lifetime) than the parent terbium polyoxometalates, and their respective hybrids show similar tendency. The quantum efficiencies of europium polyoxometalates, which are the co-contribution of all lanthanide pieces in hybrids can reach above 80%, surpassing that of parent europium polyoxometalates (52%). The quantum efficiencies of terbium polyoxometalates hybrids are above 10%, which also show outstanding luminous properties.

Furthermore, on the basis of emission spectra, the CIE chromaticity diagrams of the eight hybrids are obtained and shown in Fig. 6. The *x* and *y* coordinates of CIE are listed in Table 1. Among the eight hybrids, EuW10-IL-Eu-phen hybrid can emit red light, and EuW10-IL-Tb-bpy/TbW10-IL-Eu-bpy are located at orange light region. Other hybrid TbW10-IL-Eu-phen emits yellowish-green light under excitation. EuW10-IL-Tb-phen, EuW10-IL-Tb-bpy, TbW10-IL-Tb-phen and TbW10-IL-Tb-phen can emit white light when they are excited, showing superior white light integration properties.

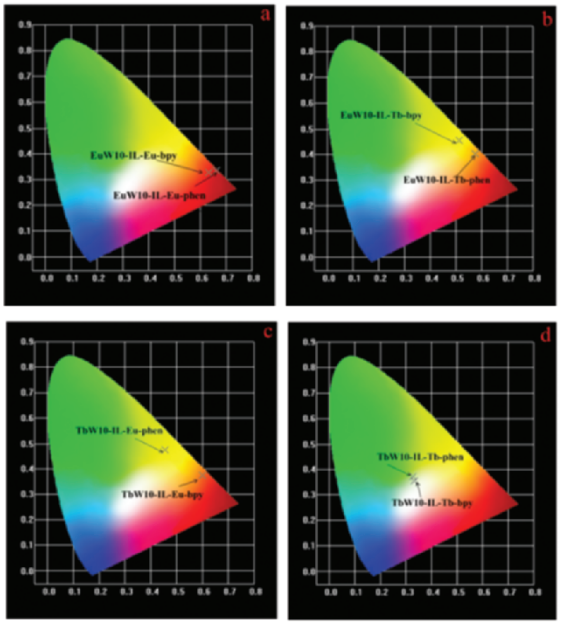

Fig. 6 The CIE chromaticity diagrams of the eight hybrids LnW10-IL-Ln′-L (Ln = Eu, Tb; Ln′ = Eu, Tb; L = phen, bpy).

Conclusion

In summary, eight kinds of task-specified ionic liquid encapsulating lanthanide polyoxometalates and coordination compounds co-assembled luminescent hybrid materials are prepared by convenient synthesis routes. Europium and terbium ions behave as a bridge to connect the carboxyl ionic liquid/polyoxometalates part with organic ligand (bpy or phen) to assemble luminescent hybrid. The results of structural analysis tell us that all hybrid materials are amorphous structures, indicating that no free polyoxometalates salts or lanthanide inorganic compounds exist. This proves that all these inorganic building blocks are assembled into the hybrids by chemical bonds, and the whole system is in a more homogeneous phase. The luminescent decay lifetime of most novel luminescent hybrids can reach millisecond level, and that of the hybrids encapsulating europium polyoxometalates is higher than terbium polyoxometalates assembled hybrids. The quantum efficiency of europium polyoxometalates is also

Table 1 The data of quantum efficiency, *x*/*y* coordinates of CIE

Hybrid materials	τ [a]/μs	η/%	*x*	*y*	λ_{ex}/nm	Color
EuW10-IL-Eu-phen	1095	83	0.6623	0.3343	350	Red
EuW10-IL-Eu-bpy	590	86	0.6329	0.3283	316	Orange
EuW10-IL-Tb-phen	1084[b]	92	0.5759	0.4016	336	Nearly white
EuW10-IL-Tb-bpy	1258[b]	90	0.513	0.4538	318	Nearly white
TbW10-IL-Eu-phen	892[b]	12	0.4553	0.4747	350	Greenish-yellow
TbW10-IL-Eu-bpy	448[b]	22	0.5989	0.3751	378	Orange
TbW10-IL-Tb-phen	1064	47	0.3321	0.3556	330	White
TbW10-IL-Tb-bpy	332	29	0.3279	0.3732	378	White

[a] Decay lifetimes of $^5D_0(Eu^{3+})$ and $^5D_4(Tb^{3+})$ excited state. [b] The data in table are the decay lifetimes of $^5D_0(Eu^{3+})$ and their data of $^5D_4(Tb^{3+})$ excited state are 169, 1132, 384 and 486 μs, respectively.

excellent, and EuW10-IL-Tb-phen possesses the highest quantum efficiency, which can reach 92%. Among all obtained hybrids, EuW10-IL-Tb-phen, EuW10-IL-Tb-bpy, TbW10-IL-Tb-phen, TbW10-IL-Tb-bpy can emit high quality white light that have great potential in white light devices.

Acknowledgements

This work was supported by the National Natural Science Foundation of China (91122003) and the Developing Science Funds of Tongji University.

Notes and references

1 (*a*) C. X. Li and J. Lin, *J. Mater. Chem.*, 2010, **20**, 6831; (*b*) K. Kuriki, Y. Koike and Y. Okamoto, *Chem. Rev.*, 2002, **102**, 2347.

2 (*a*) J. Silver and R. Withnall, *Chem. Rev.*, 2004, **104**, 2833; (*b*) J. Kido and Y. Okamoto, *Chem. Rev.*, 2002, **102**, 2357; (*c*) Z. G. Chen, H. L. Chen, H. Hu, M. X. Yu, F. Y. Li, Q. Zhang, Z. G. Zhou, T. Yi and C. H. Huang, *J. Am. Chem. Soc.*, 2008, **130**, 3023.

3 S. Bruck, M. Hilder, P. C. Junk and U. H. Kynast, *Inorg. Chem. Commun.*, 2000, **3**, 666.

4 D. Parker and J. A. G. Williams, *J. Chem. Soc., Dalton Trans.*, 1996, 3613.

5 (*a*) D. M. Wang, J. H. Zhang, Q. Lin, L. S. Fu, H. J. Zhang and B. Yang, *J. Mater. Chem.*, 2003, **13**, 2279; (*b*) F. Wang, D. Banerjee, Y. S. Liu, X. Y. Chen and X. G. Liu, *Analyst*, 2010, **135**, 1839.

6 (*a*) J. S. Wang, Z. W. Wang, X. Li, S. Wang, H. D. Mao and Z. J. Li, *Appl. Surf. Sci.*, 2011, **257**, 7145; (*b*) B. Yan, M. Guo and X. F. Qiao, *Photochem. Photobiol.*, 2011, **87**, 786.

7 (*a*) K. Binnemans, *Chem. Rev.*, 2009, **109**, 4283.

8 (*a*) S. Yanagida, Y. Hasegawa, K. Murakoshi, Y. Wada, N. Nakashima and T. Yamanaka, *Coord. Chem. Rev.*, 1998, **171**, 461; (*b*) G. F. de Sa, O. L. Malta, C. D. Donega, A. M. Simas, R. L. Longo, P. A. Santa-Cruz and E. F. da Silva, *Coord. Chem. Rev.*, 2000, **196**, 165; (*c*) D. J. Wang, Y. Pi, C. Y. Zheng, L. Fan, Y. J. Hu and X. H. Wei, *J. Alloys Compd.*, 2013, **574**, 54.

9 J. Zhang, W. X. Li, B. Y. Ao, S. Y. Feng and X. D. Xin, *Spectrochim. Acta, Part A*, 2014, **118**, 972.

10 (*a*) J. Feng and H. J. Zhang, *Chem. Soc. Rev.*, 2013, **42**, 387; (*b*) W. Bo and M. H. Zhu, *Inorg. Chem. Commun.*, 2000, **3**, 243.

11 M. Mirzaei, H. Eshtiagh-Hosseini, N. Lotfian, A. Salimi, A. Bauza, R. Van Deun, R. Decadt, M. Barcelo-Oliver and A. Frontera, *Dalton Trans.*, 2014, **43**, 1906.

12 (*a*) Y. Jia, H. Q. Tan, Z. M. Zhang and E. B. Wang, *J. Mater. Chem. C*, 2013, **1**, 3681; (*b*) A. Nisar, J. Zhuang and X. Wang, *Adv. Mater.*, 2011, **23**, 1130; (*c*) T. Ito, H. Yashiro and T. Yamase, *Langmuir*, 2006, **22**, 2806; (*d*) W. F. Bu, L. X. Wu, X. Zhang and A. C. Tang, *J. Phys. Chem. B*, 2003, **107**, 13425.

13 E. D. Bates, R. D. Mayton, I. Ntai and J. H. Davis, *J. Am. Chem. Soc.*, 2002, **124**, 926.

14 Y. Mei, Y. Lu and B. Yan, *New J. Chem.*, 2013, **37**, 2619.

15 J. H. Olivier, F. Camerel, J. Selb, P. Retailleau and R. Ziessel, *Chem. Commun.*, 2009, 1133.

16 (*a*) J. F. Dubreuil and J. P. Bazureau, *Tetrahedron Lett.*, 2000, **41**, 7351; (*b*) P. Nockemann, B. Thijs, K. Lunstroot, T. N. Parac-Vogt, C. Gorller-Walrand, K. Binnemans, K. Van Hecke, L. Van Meervelt, S. Nikitenko, J. Daniels, C. Hennig and R. Van Deun, *Chem. – Eur. J.*, 2009, **15**, 1449.

17 Q. P. Li and B. Yan, *Dalton Trans.*, 2012, **41**, 8567.

18 (*a*) R. D. Peacock and T. J. R. Weakley, *J. Chem. Soc. A*, 1971, 1836; (*b*) J. Wang, F. Y. Liu, L. S. Fu and H. J. Zhang, *Mater. Lett.*, 2002, **56**, 300; (*c*) C. M. Granadeiro, R. A. S. Ferreira, P. C. R. Soares-Santos, L. D. Carlos and H. I. S. Nogueira, *J. Alloys Compd.*, 2008, **451**, 422.

19 H. R. Li, D. Li, Y. G. Wang and Q. R. Ru, *Chem – Asian J.*, 2011, **6**, 1443.

20 D. T. M. Hoa, H. S. Kim, B. J. Lee, D. H. Park and Y. S. Kwon, *Curr. Appl. Phys.*, 2006, **6**, 605.

21 (*a*) H. M. Ye, N. Ren, J. J. Zhang, S. J. Sun and J. F. Wang, *Struct. Chem.*, 2010, **21**, 165; (*b*) J. R. Zheng, N. Ren, J. J. Zhang, D. H. Zhang, L. Z. Yan and S. P. Wang, *J. Chem. Thermodyn.*, 2013, **57**, 169.

22 X. Liu, J. Jiang, Y. Guo, S. Yong, K. Yang and L. Nie, *Rare Met.*, 2012, **31**, 484.

23 K. Lunstroot, K. Driesen, P. Nockemann, C. Gorller-Walrand, K. Binnemans, S. Bellayer, J. Le Bideau and A. Vioux, *Chem. Mater.*, 2006, **18**, 5711.

24 K. Lunstroot, K. Driesen, P. Nockemann, K. Van Hecke, L. Van Meervelt, C. Gorller-Walrand, K. Binnemans, S. Bellayer, L. Viau, J. Le Bideau and A. Vioux, *Dalton Trans.*, 2009, 298.

25 (*a*) L. Guo, B. Yan and J. L. Liu, *Dalton Trans.*, 2011, **40**, 4933; (*b*) S. Mallakpour and M. Dehghani, *Synth. React. Inorg. Met.*, 2014, **44**, 235.

26 A. Bellusci, G. Barberio, A. Crispini, M. Ghedini, M. La Deda and D. Pucci, *Inorg. Chem.*, 2005, **44**, 1818.